

DJ-1 Is a Copper Chaperone Acting on SOD1 Activation*

Received for publication, November 18, 2013, and in revised form, February 7, 2014. Published, JBC Papers in Press, February 24, 2014, DOI 10.1074/jbc.M113.535112

Stefania Girotto^{‡§}, Laura Cendron^{¶||}, Marco Bisaglia^{||}, Isabella Tessari^{||}, Stefano Mammi[‡], Giuseppe Zanotti[¶], and Luigi Bubacco^{||1}

From the [‡]Department of Chemical Sciences, University of Padova, via Marzolo, 1 35131 Padova, Italy, [§]Department of Drug Discovery and Development, Istituto Italiano di Tecnologia, Via Morego, 30 16163 Genoa, Italy, and the Departments of [¶]Biomedical Sciences and ^{||}Biology, University of Padova, Via Ugo Bassi, 58b 35121 Padova, Italy

Background: DJ-1 and SOD1 are proteins involved in Parkinson disease and ALS, respectively.

Results: A novel DJ-1 copper binding site is characterized together with its ability to activate SOD1 through copper transfer.

Conclusion: We have identified a putative role for DJ-1 as a copper chaperone.

Significance: Alterations of the coordination of the copper ion in DJ-1 may affect neurodegenerative etiopathogenesis.

Lack of oxidative stress control is a common and often prime feature observed in many neurodegenerative diseases. Both DJ-1 and SOD1, proteins involved in familial Parkinson disease and amyotrophic lateral sclerosis, respectively, play a protective role against oxidative stress. Impaired activity and modified expression of both proteins have been observed in different neurodegenerative diseases. A potential cooperative action of DJ-1 and SOD1 in the same oxidative stress response pathway may be suggested based on a copper-mediated interaction between the two proteins reported here. To investigate the mechanisms underlying the antioxidative function of DJ-1 in relation to SOD1 activity, we investigated the ability of DJ-1 to bind copper ions. We structurally characterized a novel copper binding site involving Cys-106, and we investigated, using different techniques, the kinetics of DJ-1 binding to copper ions. The copper transfer between the two proteins was also examined using both fluorescence spectroscopy and specific biochemical assays for SOD1 activity. The structural and functional analysis of the novel DJ-1 copper binding site led us to identify a putative role for DJ-1 as a copper chaperone. Alteration of the coordination geometry of the copper ion in DJ-1 may be correlated to the physiological role of the protein, to a potential failure in metal transfer to SOD1, and to successive implications in neurodegenerative etiopathogenesis.

DJ-1 is a protein, ubiquitously expressed predominantly in the cytosol, which has also been detected in the nucleus and in the mitochondria of some cell types (1). *PARK7*, the 24-kb gene encoding DJ-1, has been implicated as the causative gene in a familial form of Parkinson disease. Mutations in the DJ-1 gene have been associated with autosomal recessive parkinsonism, characterized by early onset and slow progression (2). It has also been suggested that DJ-1 has a pathogenic role not only in inherited cases but also in the more common sporadic form of the disease (3).

* This work was supported by Italian Ministry of Education, University and Research Grant PRIN2010-M2JARJ and University of Padova Grant PRAT2010-CPDA103503.

The atomic coordinates and structure factors (codes 4MNT, 4MTC, 4NOM, and 4N12) have been deposited in the Protein Data Bank (<http://www.pdb.org/>).

¹ To whom correspondence should be addressed. Tel.: 39-049-8276346; Fax: 39-049-8276300; E-mail: luigi.bubacco@unipd.it.

Although the well folded, compact structure of DJ-1 has been known since 2003 (4), its physiological role is still controversial. Among the several functions that have been ascribed to this protein (5), the most corroborated one is its putative neuronal protective role against oxidative stress, although how exactly this function is exerted is still unclear (6). Overexpression of wild-type DJ-1 has a neuronal cytoprotective effect against oxidative stress (7), whereas DJ-1 deficiency leads to increased vulnerability to oxidative stress-induced cell death (8). Further support for this neuronal cytoprotective function comes from the observation that the L166P DJ-1 mutation, associated with the pathology, impairs the functionality of the protein by reducing its stability (9). Clearly, this indicates that at least some mutations in DJ-1 cause a loss of function. Other DJ-1 pathological mutations result in quite stable proteins, suggesting that DJ-1 mutations lead to protein function impairment through different mechanisms.

Investigations on the oxidative stress response exerted by DJ-1 have been focused on the key role of the highly conserved Cys-106 residue. Upon exposure to reactive oxygen species, all three cysteines (Cys-46, -53, and -106) present in the sequence of DJ-1 are oxidized (10). However, only Cys-106 has a reduced pK_a value (5.4), and therefore it occurs almost exclusively as the highly reactive cysteine thiolate anion at physiological pH (11). Cys-106 has also a marked susceptibility to dopaquinone reactivity (12). A hint that cysteine 106 is responsible for the “signaling” role of DJ-1 in coordinating cellular responses to oxidative stress is the observation that mutation of this residue exacerbates cell sensitivity toward oxidative stress. These data have been supported by the finding of unusually high levels of acidic forms of DJ-1 in brain samples of Parkinson disease patients, compared with the distribution of DJ-1 pI isoforms usually observed in normal brains (13). It has also been proved that oxidation of Cys-106 has a different but most likely complementary role, which is its ability to drive and control DJ-1 mitochondrial localization (7).

Multiple literature reports underline the indisputable co-participation of DJ-1 and copper-zinc superoxide dismutase ($\text{Cu}_2\text{Zn}_2\text{SOD1}$ or SOD1)² in the complex pathways of cellular

² The abbreviations used are: SOD, superoxide dismutase; CCS, copper chaperone for SOD1.

DJ-1 Is a Copper Chaperone Acting on SOD1 Activation

oxidative stress response (14, 15). *In vivo*, SOD1 is the first line of defense against reactive oxygen species, scavenging superoxide radicals (16). Altered SOD1 activity has been associated with different pathologies (17) and in particular with motor neuron degeneration, such as in both sporadic and familial cases of amyotrophic lateral sclerosis (18).

SOD1 is a metalloenzyme that catalyzes the disproportionation of superoxide to give molecular oxygen and hydrogen peroxide. The enzyme contains two identical subunits of 153 amino acids, each one built around a β -barrel core plus several long loops of irregular structure. Each subunit contains a metal binding region that binds one copper and one zinc ion, positioned such that they share a common histidyl imidazolate ligand when the copper ion is present as Cu(II). The copper ion has a catalytic function, whereas the zinc ion has a structural role. The metal ions have an enormous effect on the thermal stability of SOD1. The binding of metal ions also increases the affinity of the two subunits within the protein dimer and decreases the susceptibility to proteolysis relative to that of apo-SOD1 (19).

In 2011, Wang *et al.* (20) suggested that DJ-1 is able to control oxidative stress insults by indirectly regulating SOD1 expression through the Erk1/2-Elk1 pathway. They demonstrated that upon oxidative insults, DJ-1 interacts with Erk1/2, and it determines its nuclear translocation. The translocation of Erk1/2 then activates Elk1 and sequentially promotes SOD1 expression.

One of the proposed mechanism for oxidative stress protection activated by DJ-1 hinges on the idea that DJ-1 control takes place through a direct interaction of DJ-1 with cytosolic SOD1 in a copper-dependent mode (21). Mainly through isothermal titration calorimetry and bimolecular fluorescence complementation assays, Xu *et al.* (22) showed that an *Arabidopsis thaliana* DJ-1 homolog is able to bind Cu(II) and to interact directly with SOD1. More recently, the same authors showed, through x-ray fluorescence, that human DJ-1 is able to bind both mercury and copper ions. DJ-1 metal binding ability is associated with a potential protective function of DJ-1 against metal-induced cytotoxicity, suggesting that DJ-1 is sequestering extra copper in conditions of metal dyshomeostasis.

To investigate the mechanisms underlying the antioxidative function of DJ-1 in relation to SOD1 activity, we engaged in the structural characterization of a DJ-1 copper binding site using different techniques. We further characterized the kinetic ability of DJ-1 to bind copper ions, which led us to identify a putative role of DJ-1 as a copper metallochaperone. The results presented here suggest a functional implication of the DJ-1 metal binding site; alteration of its geometry of coordination may be correlated to the physiological role of the protein and to the etiopathogenesis of Parkinson disease.

EXPERIMENTAL PROCEDURES

DJ-1 Expression and Purification—Human wild-type DJ-1 cDNA was amplified by PCR using the pcDNA3.1/GS-DJ-1 vector, containing the full-length DJ-1 coding region as template (a generous gift of Dr. M. R. Cookson), and synthetic oligonucleotides (Sigma-Genosys) containing the NcoI and XhoI restriction sites. After digestion with the appropriate restric-

tion enzymes, the PCR product was subcloned into the NcoI-XhoI linearized pET28 expression plasmid (Novagen) and introduced into *Escherichia coli* BL21(DE3) strain. The C106A, C53A, H126A, H126Q, E18D, and E18Q mutants were generated by site-directed mutagenesis using specific oligonucleotides. Overexpression of the proteins was achieved in *E. coli* BL21(DE3) strain, by growing cells in LB medium at 37 °C to an A_{600} of 0.6, followed by induction with 0.6 mM isopropyl β -D-thiogalactopyranoside for 4–5 h. After sonication and centrifugation, the soluble fraction, containing DJ-1, was subjected to a two-step (70 and 90%) ammonium sulfate precipitation. The pellet was then resuspended, dialyzed against 20 mM Tris-HCl, pH 8.0, 3 mM dithiothreitol (DTT), and purified through a 6-ml Resource Q column (Amersham Biosciences). After purification, wild-type DJ-1 and its mutants were stored at 4 °C in 20 mM Tris-HCl, pH 8.0, 10 mM DTT for no more than 2 weeks. Protein concentration was estimated using the extinction coefficient of the monomeric DJ-1 form, $\epsilon_{280} = 4200 \text{ M}^{-1} \text{ cm}^{-1}$.

SOD1 Expression and Purification—Human SOD1 cDNA, purchased by Source BioScience imaGenes, was subcloned into the NcoI and XhoI restriction sites of the pET15b plasmid (Novagen). The protein was expressed in *E. coli* MnSOD/FeSOD^{-/-} QC774(DE3) strain (23) to eliminate a possible interference of the endogenous proteins with the recombinant one. This mutant strain was generously provided by Prof. A. F. Miller (University of Kentucky, Lexington, KY).

SOD1 was recovered from the periplasm by osmotic shock as described previously (24). Then the soluble fraction, containing SOD1, was subjected to a two-step (70 and 95%) ammonium sulfate precipitation. The pellet was then resuspended, dialyzed against 20 mM Tris-HCl, pH 8.0, 1 mM DTT, loaded into a 6-ml Resource Q column (Amersham Biosciences), and eluted with a 0–500 mM gradient of NaCl. Protein concentration was spectroscopically evaluated using the extinction coefficient $\epsilon_{256} = 15,900 \text{ M}^{-1} \text{ cm}^{-1}$, corresponding to the dimer (25).

The apoprotein was obtained by dialysis against 10 mM EDTA in 50 mM acetate buffer, pH 3.8 (26). EDTA was removed by dialysis against 100 mM NaCl in 50 mM acetate buffer, pH 3.8, and then against acetate buffer alone, gradually increasing the pH from 3.8 to 5.5 (27). Finally, the E₂Zn₂·SOD1 was obtained by adding a ZnCl₂ solution to the apoprotein at pH 5.5.

Crystallization and Data Collection—Purified samples of wild type recombinant DJ-1 in complex with Cu(II) ions were submitted to sparse matrix crystallization trials, applying the isothermal vapor diffusion method, partially automated by Oryx8 Robot (Douglas Instruments). Each of the 384 independent crystallization conditions tested (Crystal screen I and II, PACT screen, PEGs II screen, and PGA screen) were screened using the sitting drop set up on MRC 2-well plates. Prior to crystallization, the freshly purified protein was titrated with 0.1 M Cu(II)·SO₄ solution (monomer/copper ion = 1:1 ratio) and subsequently concentrated to 0.8–1 mM under anaerobic conditions.

Diffraction quality crystals grew in more than 20 different conditions, which were screened in order to identify those more suitable for the crystallization of the Cu·DJ-1 complex and dis-

TABLE 1

X-ray diffraction information

Collection and refinement statistics of the x-ray data acquired at 100 K at both the Swiss Light Source (Villigen, Switzerland) and European Synchrotron Radiation Facility (Grenoble, France) are shown. Data for the highest resolution shell are shown in parentheses.

	WT DJ1-Cu	E18D DJ1-Cu	C53A DJ1-Cu	C53A DJ1
Data collection				
Wavelength (Å)	1.378	1.370	1.378	1.378
Space group, Z	P ₃ ₁ 2 ₁ 1			
a = b, c (Å)	75.24, 75.30	75.49, 75, 78	75.14, 75.27	75.22, 75.64
Resolution (Å)	24.64–1.58 (1.67–1.58)	29.86–1.478 (1.56–1.478)	33.62–1.95 (2.06–1.95)	37.82–1.47 (1.55–1.47)
No. of unique reflections	33,930 (4871)	41,496 (5696)	18,268 (2617)	42,517 (6162)
R _{merge}	0.063 (0.292)	0.08 (0.185)	0.114 (0.351)	0.096 (0.419)
$\langle I/\sigma(I) \rangle$	7.5 (2.6)	5.1 (3.7)	4.7 (1.7)	4.0 (1.6)
Completeness (%)	99.9 (99.8)	99.9 (100)	99.6 (100)	99.8 (100)
Anomalous completeness (%)	100 (99.9)	99.8 (100)	99.6 (100)	99.6 (99.9)
Multiplicity	15.5 (14.8)	11.2 (11.1)	8.2 (8.2)	10.3 (10.3)
Anomalous multiplicity	8.0 (7.6)	5.7 (5.6)	4.2 (4.2)	5.2 (5.0)
Refinement				
R _{work} /R _{free} (%)	15.66/17.80	16.32/17.31	14.59/18.37	16.15/16.56
No. of atoms				
Protein	1379	1404	1392	1398
Solvent (H ₂ O, etc.)	264	169	179	229
Copper ions	2	1	1	
Root mean square deviations				
Bond lengths (Å)	0.008	0.006	0.007	0.006
Bond angles (degrees)	1.09	1.163	1.06	1.14
Mean B value (Å ²)	16.40	16.67	20.27	17.67

card those where any of the precipitant components could act as a chelating agent and aid to Cu(II) stripping.

In the best conditions, pale green regular crystals grew within 24–48 h by mixing equal volumes of Cu·DJ-1 adduct and a precipitant solution, consisting of 0.2 M sodium malonate and 20% (w/v) PEG 3350 (Molecular Dimension Ltd.), left equilibrating at 293 K against 450 μ l of the same solution in the reservoir well. The crystals were reproduced and optimized on 24-well Linbro-style plates (Molecular Dimension Ltd.) under anaerobic conditions (glove box MBRAUN MB 200B), using O₂-free solutions.

C53A DJ-1 mutant in complex with Cu(II) was prepared and crystallized using the same method and precipitant solutions of the wild type protein, with small adjustments of the protein and precipitant concentrations. Crystals of C53A DJ-1 mutant were grown also in the absence of copper but under identical conditions, to analyze the changes occurring upon copper binding. At variance, the copper adduct of E18D DJ-1 was prepared by soaking apo-crystals, grown under anaerobic conditions and with the same precipitant, by transferring the same ones in a fresh drop of precipitant supplemented with 1 mM CuSO₄. Before data collection, the crystals were quickly soaked into a cryoprotectant solution composed of the precipitant agent, supplemented with 20% (v/v) ethylene glycol, and flash-frozen in liquid nitrogen.

X-ray diffraction data were collected at 100 K both at the Swiss Light Source (Villigen, Switzerland) and the European Synchrotron Radiation Facility (Grenoble, France) synchrotron radiation sources (see details in Table 1). Any of the data collections were acquired around the absorption peak of copper ions (~1.47 Å) to obtain the corresponding anomalous signal.

Diffraction data were processed using iMosflm, and integrated intensities were scaled using software Scala, with the ccp4i package interface (28). Data collection statistics are summarized in Table 1. All of the crystals diffracted to a resolution higher than 2.0 Å, ranging from 1.95 to 1.35 Å in the best case.

Both the WT and DJ-1 mutant crystals, either in complex with copper ions or not, belong to the trigonal P₃₁2₁ space group, with one molecule per asymmetric unit, a solvent content of 56%, and unit cell parameters very close to each other and to the first structure of DJ-1, crystallized in the same space group but starting from different precipitant agents (Protein Data Bank codes 1P5F (4) and 1SOA (7)).

Model Building and Refinement—The structure was solved by molecular replacement using the software autoMR, part of the PHENIX suite (29), starting from the structure of DJ-1 protein solved by Wilson and co-workers (Protein Data Bank code 1SOA (7)). The refinement was carried out using the software phenix.refine (29) and Refmac5 (30). A few steps of manual rebuilding, performed with the graphic software Coot (31), were sufficient to verify and introduce the appropriate mutations and obtain the final models. Solvent molecules were identified by an automated procedure feasible in the phenix.refine options and small manual adjustments. Copper ions were placed by inspecting the anomalous difference maps. A residual electron density that could not be ascribed to any protein residues or solvent was observed in the structures of mutants Cu·E18D and apo-C53A roughly in the same position, in the pocket that hosts the copper binding site involving Cys-106. This density has been tentatively fitted by a molecule of ethylene glycol, added as cryoprotectant before data collection. An analogous electron density is observed in the structure of the copper-loaded C53A mutant, where it is however shifted 5 Å apart, toward a more peripheral side of the pocket. The final models content as well as the corresponding quality and geometry parameters, falling in the expected range or better for this resolution, are briefly summarized in Table 1. The only residue that invariably fell into generously allowed regions of the Ramachandran plot was cysteine 106, and this was most likely due to chemical modification that it undergoes, as described below.

UV-visible Titration—Copper titrations were performed on 0.2 mM protein samples with 1- μ l additions of a stock solution

DJ-1 Is a Copper Chaperone Acting on SOD1 Activation

(10 mM) of $\text{CuSO}_4 \cdot 5\text{H}_2\text{O}$. UV-visible titrations were performed on an Agilent 8453 UV-visible spectroscopy system at room temperature in the 200–1100 nm range. All spectra were blanked against phosphate buffer at the appropriate pH.

In order to test the pH-dependent shift of the copper charge transfer band, different aliquots of the same DJ-1 stock solution were extensively dialyzed against phosphate buffers at different pH values. Protein concentration and successive titration with $\text{CuSO}_4 \cdot 5\text{H}_2\text{O}$ according to the above described protocol were then carried out for each protein sample at different pH values.

Fluorescence Titration—Fluorescence spectra of metal-free SOD1 protein were initially recorded using a Varian Cary Eclipse fluorescence spectrophotometer.

The exploited probe to test copper transfer from Cu(II)-DJ-1 to $\text{E}_2\text{Zn}_2\text{SOD1}$ was Trp-32, the only tryptophan residue present in SOD1. Although this residue is solvent-exposed, its fluorescence emission is influenced by the protein matrix. DJ-1 has no tryptophan residues in its sequence but only three tyrosine residues, the intrinsic fluorescence of which is negligible.

The excitation wavelength was 280 nm (bandwidth 5 nm), and the fluorescence emission was collected between 300 and 460 nm (bandwidth 10 nm). Fluorescence spectra were recorded, at room temperature, after the sequential addition of concentrated (850 μM) copper-loaded DJ-1 protein directly into the quartz cuvette containing the apo-SOD1 protein (4 μM dimeric concentration). Spectra were also recorded 10 and 20 min after mixing in order to detect the mixture at equilibrium. After stoichiometric titration, the further addition of 0.5 eq of copper showed only a further 3% decrease of SOD1 fluorescence, confirming that a complete transfer of the copper ion had taken place from WT DJ-1 to $\text{E}_2\text{Zn}_2\text{SOD1}$.

EPR Spectroscopy—The EPR spectra were recorded at 77 K with an X-band Bruker Elexsys E580 spectrometer. 300 μl of copper-loaded DJ-1 samples (790 μM) were loaded into a 4-mm diameter iron-free quartz EPR tube. Before recording the spectra, samples were degassed at room temperature. Spectra were collected using the following spectrometer settings: high power (3.5 db), high modulation amplitude (5 G), and wide scan range (4000 G).

Peroxiredoxin Activity—DJ-1 peroxiredoxin activity was measured using an Amplex[®] Red hydrogen peroxide/peroxidase assay kit containing a one-step assay that uses the Amplex[®] Red reagent (10-acetyl-3,7-dihydroxyphenoxazine) to detect hydrogen peroxide.

The assay was based on the spectrophotometric detection of resorufin absorbance at 560 nm ($\epsilon = 58,000 \text{ cm}^{-1} \text{ M}^{-1}$). Resorufin is the red fluorescent oxidation product obtained from the reaction of Amplex[®] Red reagent with H_2O_2 in a 1:1 stoichiometry in the presence of horseradish peroxidase (HRP). The H_2O_2 scavenging activity of DJ-1 was monitored as the decrease of resorufin absorbance detected in the presence of the protein compared with the control (*i.e.* the same reaction mixture in the absence of DJ-1). All of the experiments were performed with 10 μM H_2O_2 , which was initially chosen as the optimal concentration for the experiment. A calibration curve was run using different concentrations of H_2O_2 . Samples were prepared in a 96-well microplate, and the absorbance was detected using a

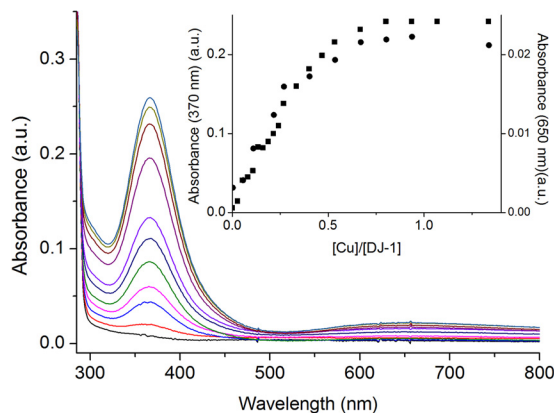


FIGURE 1. UV-visible absorption curves recorded for the WT DJ-1 protein upon titration with Cu(II) . Inset, comparison of the variation of the charge transfer band (370 nm; ■) and of the d-d transition band (650 nm; ●) observed upon titration of WT DJ-1 protein with Cu(II) , as a function of the copper/protein ratio. *a.u.*, absorbance units.

PerkinElmer VICTOR[™] X3 2030 multilabel plate reader. Reported data are the average of three replicates.

SOD1 Activity Assays—SOD activities were determined through the cytochrome *c* assay (26) in the absence and presence of apo- or copper-loaded DJ-1 proteins (1:1 molar ratio). The reduction rate of cytochrome *c* by O_2^- radicals was monitored at 550 nm, utilizing xanthine-xanthine oxidase as a source of superoxide. The reaction mixture consisted in 50 mM potassium phosphate, pH 7.8, 0.1 mM EDTA, 50 μM xanthine, 10 μM cytochrome *c* in the absence (control) or in the presence of different amounts of SODs, in a total volume of 1 ml. After the addition of ~ 3 milliunits of xanthine oxidase, spectra were acquired every 10 s for a total period of 4 min. Each kinetic was performed in triplicate. Percentage inhibition was calculated as follows.

$$\% \text{ inhibition} = ((\text{control rate} - \text{sample rate}) / \text{control rate}) \times 100 \quad (\text{Eq. 1})$$

To obtain the enzymatic parameters the values calculated with different amounts of SOD (expressed in μg) have been fitted by a rectangular hyperbola,

$$y = abx / (1 + bx) \quad (\text{Eq. 2})$$

where *a* represents the maximal percentage of inhibition obtained, and *b* indicates the units/ μg of protein.

Statistical Analysis—Data were analyzed using GraphPad Prism version 4 software. One-way analysis of variance followed by Newman-Keuls's post hoc test was used to determine whether groups were statistically different. *p* values of < 0.05 were considered significant.

RESULTS

We initially performed a titration of a DJ-1 sample with Cu(II) , in which we monitored the metal binding by UV-visible spectroscopy. We observed the development of a charge transfer band in the absorption spectrum of DJ-1 at 370 nm together with a broad and weak absorption band at 650 nm (Fig. 1).

An accurate titration of a DJ-1 sample in phosphate buffer at pH 7.4 allowed us to observe that both bands at 370 and 650 nm

reached saturation when 1 eq of copper was added to the sample. However, from the titration curve, it is apparent that the stoichiometry is 0.5:1 (Fig. 1, *inset*), indicating that DJ-1 is partially loaded with copper ions because it binds 0.5 copper ions/monomer. The titration curve is typical of a simple binding event, suggesting that the binding of one copper ion to the DJ-1 dimer hinders the binding of the second metal ion. The dissociation constant (K_d) for the metal binding to the protein was determined from the titration to be 3.97×10^{-4} M with an extinction coefficient for the copper complex of $\epsilon_{370\text{ nm}} = 3300$ M⁻¹ cm⁻¹. Such a high value of the dissociation constant is compatible with a chaperone-like rather than an enzymatic function of the metalloprotein.

Further information on the potential copper-binding site was acquired through a pH dependence investigation of the position of the charge transfer band (Fig. 2). A sigmoidal dependence is observed in the pH range 6–8 (limited by protein stability) with a midpoint around pH 7.1. This dependence cannot be ascribed to the protonation of any specific binding residue but rather to the possible presence of a water ligand. To

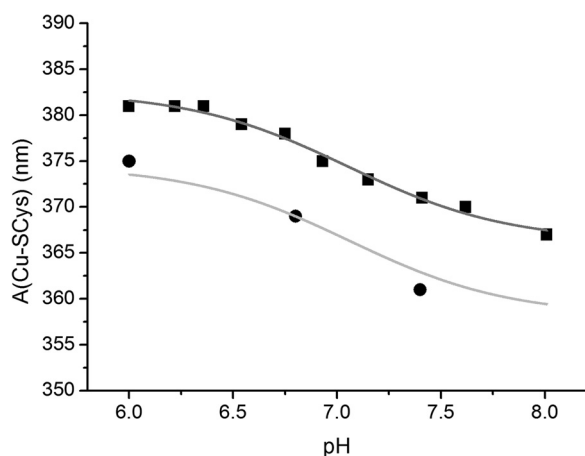


FIGURE 2. pH dependence of the charge transfer (Cu-S (Cys-106)) band for the WT (■) and H126A (●) DJ-1 proteins. The WT pH dependence data were fitted using a double Boltzmann sigmoidal function (gray line). The fitting was then vertically shifted on the H126A data (light gray line).

fully characterize the structural features of the copper-loaded DJ-1 (Cu-DJ-1) protein, we determined the crystal structures of the wild type protein both in its metal-free and copper-loaded forms.

The Cu-DJ-1 complex was prepared by titrating the diluted metal-free DJ-1 samples with CuSO₄ up to a stoichiometric ratio. After buffer exchange and concentration of the DJ-1 metal-loaded protein, we obtained a green solution suggestive of Cu(II) coordination.

The solved structure superposes well onto the already deposited structure (Protein Data Bank code 1SOA) (7) of the metal-free DJ-1 form (root mean square deviation 0.15 Å). Cys-106 has a high tendency to be oxidized to sulfinic acid (Cys-106-SO₂H), as observed in the majority of the structures deposited in the Protein Data Bank. We instead succeeded in obtaining the structure of the Cys-106-reduced DJ-1 in complex with copper by storing the protein in 10 mM DTT and removing the reductant just before protein titration and crystallization through buffer exchange using a solution extensively fluxed with oxygen-free nitrogen. Moreover, the crystallization plates were prepared under anaerobic conditions (glove box) using deoxygenated solutions to prevent Cys oxidation. Any other attempt to prevent Cys-106 oxidation failed and invariably entailed the formation of crystals without copper ions, which is in agreement with the observed inability of the oxidized protein to bind copper ions in solution (*i.e.* no charge transfer band was observed at 370 nm).

The presence of copper ions has been identified by calculating and inspecting both the difference and anomalous maps at the copper absorption edge (~ 1.37 Å) and by further comparison with the corresponding structures, solved in the same conditions but in the absence of copper. Unexpectedly, two types of metal binding sites have been identified in the wild type protein structure, one close to Cys-106 in each monomer and the other at the interface of the two monomers that associate to form the physiological dimer (Fig. 3). The latter metal binding site is located between the two Cys-53 residues that face each other. Very recently, the structure of a Cu(I)-DJ-1 complex, resulting

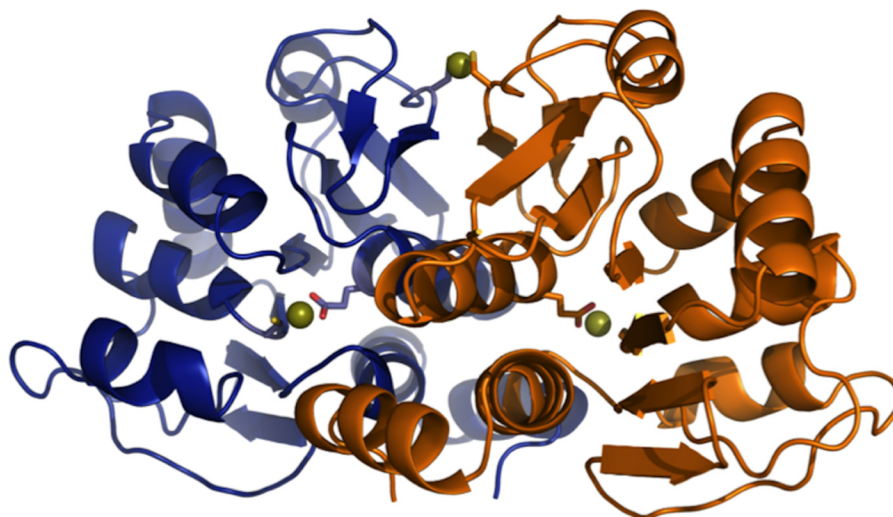


FIGURE 3. WT DJ-1 dimer with one Cu(I) binding site per monomer and a second Cu(I) binding site shared between the two monomers and located at the dimer interface.

DJ-1 Is a Copper Chaperone Acting on SOD1 Activation

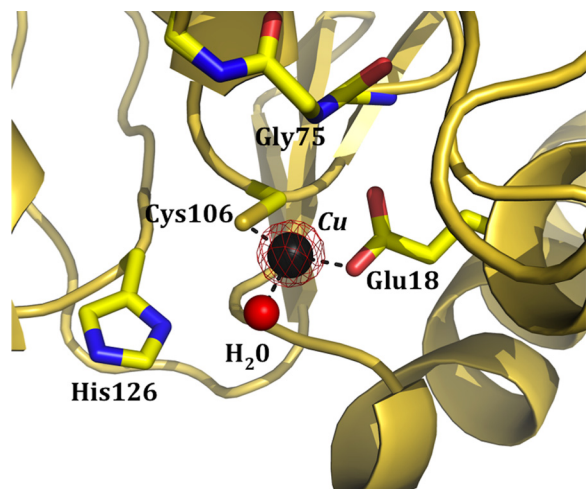


FIGURE 4. **Copper binding site 1.** Contour levels in red refer to the anomalous Fourier difference map contoured at 15σ .

from the incubation of the protein with a Cu(I)-glutathione complex, has been reported (32). In agreement with our data, the authors describe the presence of a Cu(I) ion bound at the dimer interface, whereas, at variance with us, they do not observe any metal ion bound to Cys-106. Such a discrepancy could be ascribed to the oxidation state of the copper ion, to the oxidation state of Cys-106, or to the metal binding affinity of glutathione, a well known and potent chelating agent.

Copper Coordination Site 1—A very clear peak in the anomalous difference maps, higher than 50σ , was observed in close proximity to Cys-106 of the WT DJ-1 structure and ascribed to a copper atom (Fig. 4).

The refined occupancy of the copper ion is 45–50% of the total sites in the crystal, in agreement with what was inferred from the evolution of the charge transfer band observed upon DJ-1 copper titration. The main ligands involved in the coordination of copper are two protein residues and a water molecule: Cys-106 S_{γ} atom, which points toward the copper ion at a distance of 2.09 Å; Glu-18 OE2 carboxylic oxygen, which coordinates copper at a similar distance (2.10–2.00 Å); and a water molecule at 2.32 Å.

The three ligands define roughly a trigonal geometry, where copper deviates only 0.4 Å from the Cys/Glu/ H_2O plane. The position of a fourth axial ligand is occupied by the main chain -NH of Gly-75, which nevertheless lies at a distance too large from the copper site (3.98 Å) for a coordination contribution (Fig. 4). The second carboxylic oxygen of Glu-18 side chain (OE1) is 3.26 Å away from copper, and it assumes an unfavorable geometry that seems to exclude a direct contribution to the metal coordination sphere. On the contrary, it is properly oriented (2.89 Å) to establish a hydrogen bond interaction with the main chain -NH of axial Gly-75. A further solvent molecule is positioned at 3.32 Å from the copper ion and is involved in a network of hydrogen bonds with at least other four water molecules and the side chain NH1 of Arg-48, all trapped inside the same pocket where Cys-106 is buried.

Although DJ-1 was loaded and co-crystallized with Cu(II) ions, the observed copper coordination geometry most likely corresponds to a Cu(I) complex, resulting from the photore-

duction of Cu(II) ions, which occurred during data collection. Indeed, the reducing effect of the x-ray beam on copper cannot be neglected; it has been demonstrated previously that the x-ray beam has a reducing effect on metal ions contained in crystals (33) even if cryocooled with liquid nitrogen at 100 K. Indeed, an attempt to analyze the cupric complex of DJ-1 by x-ray absorption edge spectroscopy was impaired by the immediate conversion to Cu(I) upon exposure to the x-ray beam. For these reasons, the observed copper coordination site 1 might be affected by such *in situ* metal reduction, and it could correspond to a Cu(I) complex where the metal ion is reduced and the orientation and distance of the involved ligands are consequently altered, or it configures as an intermediate and mixed state.

The copper coordination geometry described above is reminiscent of the structure of proteins belonging to the type 1 cupredoxin family (T1 sites), such as azurin or amicyanin (34, 35), in particular those characterized by a trigonal or distorted tetrahedral copper binding site (36). However, whereas DJ-1 shares the cysteine-thiolate ligand that characterizes cupredoxins, the nature of the other residues involved in the trigonal coordination arrangement of copper is not conserved. Indeed, neither histidines nor methionines seem to be involved in our case, whereas these residues are highly conserved in type 1 cupredoxins.

In the DJ-1 structure described here, the orientation of the two copper ligands (Cys-106 and Glu-18) does not undergo any significant displacement upon copper binding (see below). Indeed, the structures of both apo- and copper-loaded states of the mutant were obtained in the same crystallization conditions for the absence or presence of the metal, with the Cys-106 residue maintained in a fully reduced state in both cases. Analogous to the WT DJ-1 structure, none of the residues defining the copper binding site 1 experienced any relevant rearrangements, and only the solvent molecules trapped in close proximity to Cys-106 were reorganized upon copper binding.

Such behavior has been encountered with other cupredoxins, such as azurin. Indeed, even when Cu(II) undergoes reduction or removal from the azurin metal binding site, the structure and geometry of the corresponding coordination sphere remain almost unaffected (37). The crystallographic model described here is in agreement with the magnitude of the extinction coefficient and the energy of the optical transition described above for the Cu(II) binding site, which are indicative of a strong thiol-binding ligand.

Copper Coordination Site 2—Inspection of the anomalous difference maps of the wild type protein in complex with copper provided evidence for a second metal binding site at the homodimer interface. The metal ion is located at the interface of two asymmetric units, trapped between two cysteine residues (Cys-53), deriving from the two different chains of a DJ-1 dimer, at a distance of roughly 2.1 Å from either S_{γ} atom (Fig. 5).

This binuclear coordination is characterized by a S-Cu-S angle of about 149° , a distortion from the ideal linear dithiolate coordination that has been observed in several structures of metal-binding proteins involved in copper trafficking (38–40). The refined occupancy of such a copper ion roughly corresponds to that of copper binding site 1, which is about 45% of

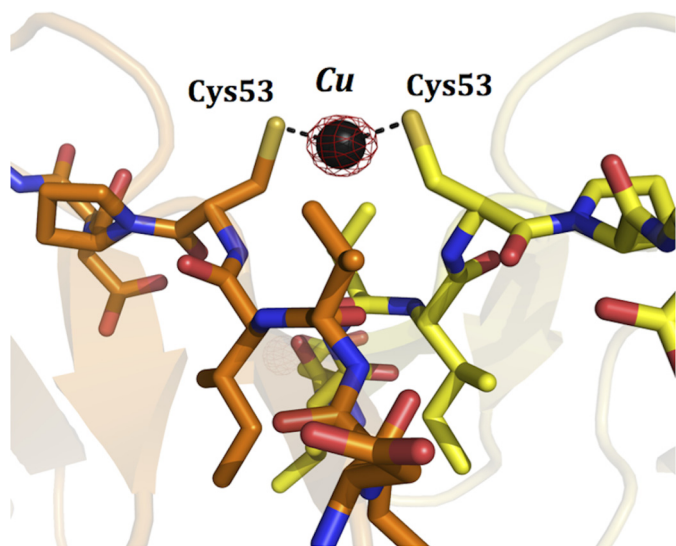


FIGURE 5. **Copper binding site 2.** Contour levels in red refer to the anomalous Fourier difference map contoured at 15σ .

the actual sites, taking into account the sharing of copper site 2 by distinct asymmetric units.

DJ-1 Mutants—The features of the newly identified copper binding sites in DJ-1 were further investigated using site-directed mutagenesis, in an attempt to validate the Cu(II) DJ-1 binding mode, which was not possible either through x-ray crystallography or x-ray absorption edge spectroscopy. Cloning, expression, and purification of the C106A DJ-1 mutant were pursued to confirm the involvement of Cys-106 in Cu(II) binding, and in fact no charge transfer absorption band was observed upon titration of the mutated DJ-1 protein with copper. This result rules out any contribution of the second copper site described above to the optical properties. In the WT protein, the involvement of Cys-106 in Cu(II) ion binding, the charge transfer band at 370 nm, and the green color of the concentrated Cu(II)-loaded protein strongly suggest a distorted tetrahedral geometry of the Cu(II) site, as already observed for the copper enzyme nitrite reductase (36). This binding hypothesis is partially supported by the Cu(I) coordination of DJ-1 observed through x-ray crystallography (see above).

Single-point mutations have been introduced also on each of the other potential copper binding ligands. Titrations with copper were performed on E18Q, E18D, H126A, H126Q, and C53A DJ-1 mutants. Moreover, the C53A and the E18D mutants were investigated through x-ray crystallography to further characterize the peculiar binding of Cu(I) at the dimer interface (see below).

The glutamic acid 18 residue was substituted with both a glutamine and an aspartic acid because it has already been shown that, whereas the E18Q mutant has a protective function against oxidative stress similar to that of the WT protein, the oxidatively impaired E18D mutant behaves as the inactive C106A mutant and fails to protect cells (41).

Upon copper titration, both DJ-1 E18D and E18Q mutants showed the formation of a charge transfer band at 370 and 365 nm (pH 6.8), respectively, that disappeared within a few minutes. These data strongly suggest that the Glu-18 is a critical residue for Cu(II) binding to DJ-1. Although only the replace-

ment of Glu-18 with Asp, and not with Gln, impairs the oxidation of Cys-106 to sulfinic acid (41), copper coordination by residue 18 is affected both by shortening of the side chain and by its charged state.

In the crystal structure of DJ-1, His-126 is located within the copper ion coordination sphere of 0.4 nm, making it a potential additional ligand for the Cu(II) ion. Nevertheless, the H126A mutation resulted in a protein with the same efficiency of copper binding as the WT DJ-1 protein. The concentration dependence in the titration data for WT and H126A are indistinguishable and representative of a non-cooperative binding. The only difference that can be observed in the binding features of the two proteins is a hypsochromic shift of about 6 nm of the charge transfer band of the H126A mutant compared with WT, which is maintained unaltered within the pH range 6.0–7.4, preserving a midpoint around pH 7.1, as reported in Fig. 2. These results suggest that the His-126 residue, even if not directly involved in copper binding, may be connected (probably by hydrogen bonding) to a binding residue affecting the coordination geometry of the site. Indeed, by inspecting the WT Cu·DJ-1 structure, we observed that His-126 imidazole ring is involved in a network of hydrogen bonds comprising also a few water molecules and other residues (Arg-28 and the CO of Pro-184) that define the copper binding pocket and belong to the second monomer of the physiological DJ-1 dimer. Mutation of His-126 to alanine induces an alteration of this extensive hydrogen bonding network, which can justify the shift of the charge transfer band observed upon copper titration of the H126A DJ-1 mutant compared with the WT protein.

An alternative mutation of the basic His-126 residue with a non-basic, similar chain length amino acid, such as Gln, resulted in binding features similar to the ones observed for E18D/E18Q mutations (*i.e.* an unstable copper binding). These data further confirm the indirect involvement of residue His-126 in copper binding, most likely through a hydrogen-bonding network.

The UV-visible absorption curve of the C53A DJ-1 titration with Cu(II) was indistinguishable from that of the WT protein. This result is consistent with the observed single non-cooperative charge transfer band formation, which reached saturation when 1 eq of Cu(II) was added to the WT DJ-1 protein sample. We may suggest, as substantiated by functional data described below, that copper coordination site 1, identified by x-ray crystallography and involving Cys-106, is more likely the functional copper chaperone binding site of DJ-1 competent to bind both Cu(I) and Cu(II).

Further confirmation that Cys-106 is the main Cu(II) binding site comes from the EPR spectra recorded on both WT Cu·DJ-1 and Cu·C53A DJ-1 samples, which are superimposable (Fig. 6), therefore suggesting that the Cys-53 binding site can be occupied most likely only by Cu(I).

An initial continuous wave EPR spectrum, which fully accounts for the metal ions added, was recorded for the WT protein loaded with copper. The spectrum revealed the simultaneous presence of two copper species. A Cu(II) species at $g_{\perp} = 2.25$ with a hyperfine splitting of 148 G was superimposed onto a second species at $g_{\perp} = 2.22$ with a hyperfine splitting of 180 G (Fig. 6). The heterogeneous Cu(II) coordination,

DJ-1 Is a Copper Chaperone Acting on SOD1 Activation

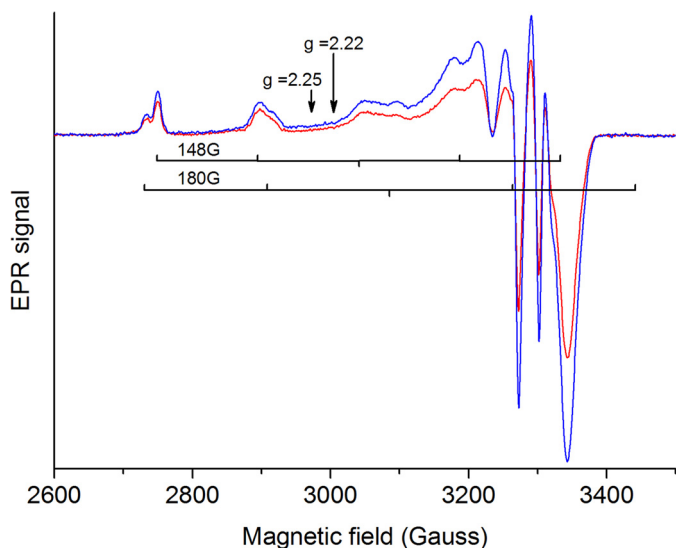


FIGURE 6. Continuous wave EPR spectrum of Cu(II)-loaded WT DJ-1 (red) and Cu(II)-loaded C53A DJ-1 (blue).

observed through EPR spectroscopy, may be due to a partial occupancy of the coordinating water molecule, a distribution that may be affected by sample freezing in liquid nitrogen. From the EPR spectra, we can infer that the paramagnetic properties of the bound Cu(II) are consistent with the coordination mode defined from the optical transitions and from the crystallographic data, assuming that no extensive rearrangement of the metal ligands occurs upon copper oxidation.

The data presented here support the purported role of DJ-1 as a redox-sensing protein in the cell. DJ-1 shows a complex, structurally modulated, redox state for the binding of Cys-106 most likely tuned by the specific side chains of the residues surrounding the copper binding site or binding of another protein partner to DJ-1.

To have a robust validation of the model that emerged from the data presented above, we pursued the structural characterization also of the relevant DJ-1 mutants in the presence of the bound copper ion. We succeeded in determining the crystal structures of the following species: apo-C53A, Cu·C53A, and Cu·E18D (Fig. 7).

All of the crystal structures described here superpose well onto each other and onto the already deposited WT DJ-1 structure (Protein Data Bank code 1SOA) (7); the root mean square deviations between equivalent $C\alpha$ atoms range from 0.15 to 0.19 Å. The only relevant difference among these structures concerns the oxidation state of the cysteines.

Although in the Cu·E18D DJ-1 mutant structure, a clear oxidation of Cys-106 to sulfinic acid (Cys-106-SO₂H) is observed, in the C53A DJ-1 mutant, Cys-106 is present in the reduced state both in the apo and copper-loaded forms. The different propensity toward Cys-106 oxidation is associated with the specific mutations that differently affect the hydrogen-bonding network that stabilizes preferentially one of the cysteine oxidation forms. The observed oxidized state of Cys-106 in mutant Cu·E18D seems to be in contrast with the impaired tendency toward oxidation detected by other authors (41) for the same mutant. However, the addition of copper ion modifies the cysteine environment, and it may thereby strongly affect the pro-

ensity of this residue toward oxidation. Nevertheless, our crystallization conditions, which differ from the one already reported for the apo form, may also have been critical in determining the Cys-106 oxidation state for this mutant. As expected, in the Cu·E18D and Cu·C53A mutant structures, a single copper ion was identified close to the binding site not affected by the mutation.

In the E18D mutant, the copper coordination site 1 is disrupted, and oxidation of Cys-106 to sulfinic acid occurred. Conversely, the copper binding site 1, the coordination geometry, and the metal occupancy are very well conserved in the Cu·C53A structure if compared with the wild type protein.

The lack of significant Cys-106 and Glu-18 orientation displacement observed in the WT protein upon copper binding was also detected for the C53A mutant. This allowed a robust validation of the Cys-106 metal binding site because both the apo- and metal-bound structures of the C53A mutant were determined in the same conditions and particularly in a fully reduced state.

As far as the second copper binding site is concerned, the peak due to the presence of a copper ion at the dimer interface and the binuclear coordination geometry are well conserved in the E18D mutant complex, whereas coordination site 1 is abolished. As expected, binding site 2 is not observed in the crystals of the Cu·C53A mutant protein.

DJ-1 Function—To address the issue of the identification of a physiological role for DJ-1 in its copper complex form, we reinvestigated a few of the many functions that have been so far ascribed to this protein.

In 2007, DJ-1 was described by Andres-Mateos *et al.* (42) as an atypical peroxiredoxin-like peroxidase. Using an Amplex® Red assay, we verified the H₂O₂ scavenging activity of recombinant WT DJ-1. Consistent with already published data (42), decreased H₂O₂ levels were observed in the presence of metal-free WT DJ-1 compared with the control reaction. The effect was concentration-dependent and reached complete peroxide scavenging when the DJ-1 monomer/H₂O₂ ratio was 1:1, therefore showing a single cysteine dependence (Fig. 8). The same experiment performed in the presence of C106A DJ-1 did not show any activity, proving that Cys-106 in DJ-1 accounts for its peroxidase-like activity (Fig. 8).

To investigate the potential role of the copper ion bound to Cys-106, the experiment was repeated in the presence of Cu·DJ-1. The results reported in Fig. 8 show that the peroxiredoxin-like activity of Cu·DJ-1 is not significantly altered compared with the metal-free WT protein, indicating that this Cys-106-related activity is not associated to the presence of copper ions.

Among the many functions ascribed to DJ-1 (5, 43), one acquires particular relevance in light of the results presented here that directly involve copper ions. According to Xu *et al.* (21), DJ-1 exerts stress control through activation and regulation of cytosolic SOD1 activity, possibly through a direct interaction of the two proteins in a copper-dependent fashion.

To evaluate the competence of DJ-1 to act as copper chaperone, we initially verified the protein's ability to transfer copper by monitoring the variation in SOD1 fluorescence induced by Cu(II)·DJ-1. A significant fluorescence quenching for the holo-

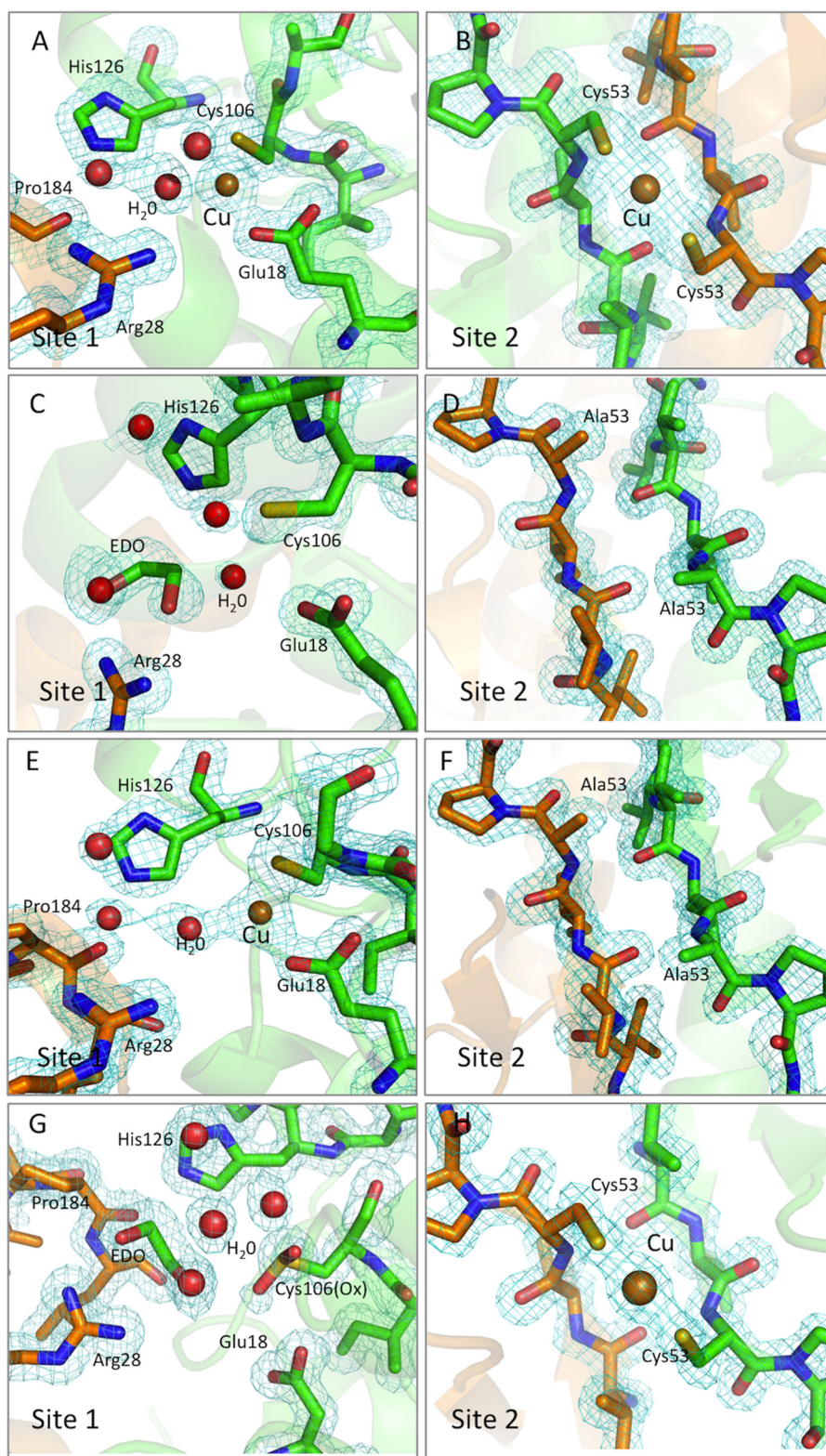


FIGURE 7. **Details of the two copper binding sites (1 and 2) identified in this work.** The panels refer to the corresponding sites in the WT and different mutant structures: WT Cu-DJ-1 (A and B), apo-C53A mutant (C and D), Cu-C53A mutant (E and F), and Cu-E18D mutant (G and H). Copper atoms are represented as orange spheres, waters are shown as red spheres.

compared with the apo-SOD1 protein has already been reported in the literature (44). Although most of the fluorescence quenching effects reported in literature are ascribed to the Cu(II) ion, it has been reported that the effect induced by

Cu(I) ion is the same as the one induced by Cu(II) ion, as for instance reported for the type 1 copper protein azurin (45).

We observed a 21 and 26% reduction of zinc-loaded E_2Zn_2 :SOD1 fluorescence intensity upon the addition of an

DJ-1 Is a Copper Chaperone Acting on SOD1 Activation

equimolar amount of WT Cu-DJ-1 and Cu-C53A DJ-1 mutant, respectively (Fig. 9), indicative of SOD1 copper loading caused by metal transfer from DJ-1. Furthermore, the decrease in SOD1 fluorescence, observed upon Cu-C53A DJ-1 addition, indicates that the presence of Cys-53 is not required for copper transfer between CuDJ-1 and E_2Zn_2 -SOD1.

To validate the suggested ability of DJ-1 to transfer copper ions to SOD1 on functional grounds, we directly measured the specific activity of the E_2Zn_2 -SOD1 enzyme in the absence and in the presence of Cu-DJ-1. SOD1 activity was determined from the percentage inhibition of the reduction rate of cytochrome *c* by O_2^- radicals. The experiment was carried out after careful removal of any aspecific copper ion from the Cu-DJ-1 solution through extensive buffer exchanges.

Fig. 10 shows that the addition of an equimolar amount of apo-DJ-1 to copper-free SOD1 does not induce significant alterations to the background activity recorded for the inactive E_2Zn_2 -SOD1. Cu-DJ-1, on the contrary, induced a significant increase in SOD1 activity (3-fold the inactive background noise).

The addition of Cu-C53A DJ-1 to copper-free SOD1 resulted in an almost 3.5-fold increase in SOD1 activity compared with

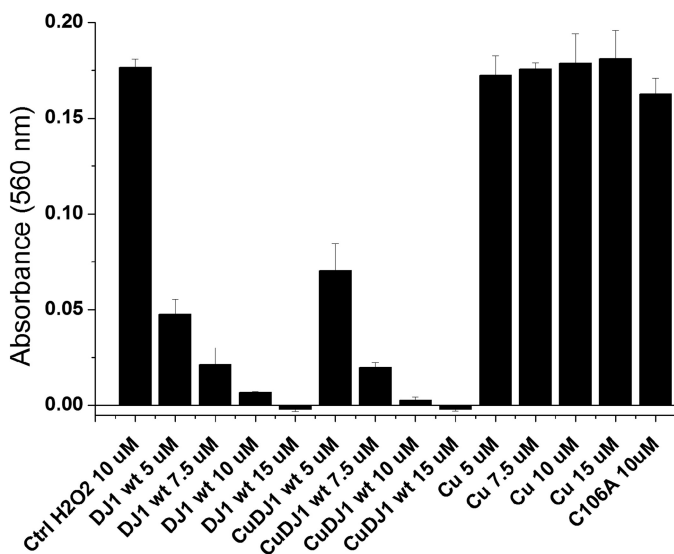


FIGURE 8. H_2O_2 scavenging activity of DJ-1 monitored as the decrease of resorufin absorbance ($A = 560$ nm). The activity was recorded in the presence of different amounts of DJ-1 in the metal-free and copper-loaded forms compared with the control and for the C106A DJ-1 mutant ($10 \mu M$). Each reported activity is the average of three replicates. Error bars, S.D.

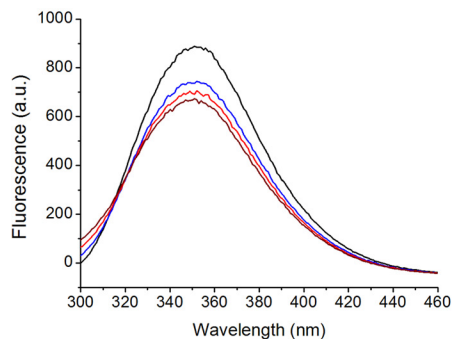


FIGURE 9. Fluorescence spectra of E_2Zn_2 -SOD1 in the absence (black) and presence of different amounts of copper-loaded WT DJ-1 (left) and copper-loaded C53A DJ-1 (right). The addition of 0.5 eq (blue), 1 eq (red), and 1.5 eq (brown) DJ-1 is shown. The fluorescence spectrum of the corresponding amount of Cu-DJ-1 in buffer was subtracted from each of the reported spectra. a.u., absorbance units.

the WT protein. The most likely explanation of this last observation is that copper is transferred to SOD1 from DJ-1 coordination site 1 and not from site 2. On the contrary, site 2 competes with SOD1 for copper, and, during the transfer of Cu(I) from DJ-1 to SOD1, part of the Cu(I) released from site 1 is transferred to site 2. When site 2 is absent, as in the case of the C53A mutant, copper from site 1 is transferred completely to SOD1. This experiment strongly supports the potential physiological role initially ascribed to DJ-1 and validates its early characterization as a copper chaperone.

DISCUSSION

In solution, DJ-1 binds Cu(II) and exhibits a green color, which originates from a (Cys-106) sulfur-copper charge transfer band. The Cu(II) binding site was characterized, and Cys-106 and Glu-18 were confirmed as ligands of the copper ion. Also, the presence of a water molecule as a ligand of the Cu(II) ion is consistent with the spectroscopic data and with the pH titration of the WT protein. The His-126 residue, an elective copper ligand in many copper proteins, in the case of DJ-1 only contributes to the second sphere coordination of the Cu(II) ion in the active site.

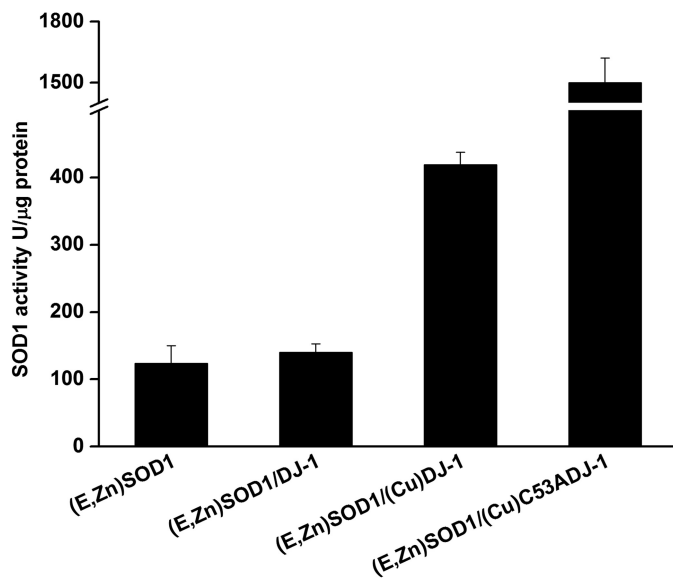


FIGURE 10. SOD1 activity, determined by using a cytochrome *c*/xanthine oxidase method, in the presence of metal-free or WT Cu-DJ-1 and Cu-C53A DJ-1. Each reported activity is the average of three replicates. Error bars, S.D.

The x-ray structure of Cu·DJ-1 showed a trigonal coordination of a Cu(I) ion located in the same site spectroscopically identified for the Cu(II) ion. Besides Cys-106, Glu-18 and a water molecule were also identified as additional ligands of the cuprous ion. A second Cu(I) binding site, the existence of which has been very recently structurally characterized (22), has been also identified. This copper binding site, which hosts only cuprous ions, consists of two Cys-53 residues belonging to the two monomers of each DJ-1 dimer.

We show, through fluorescence experiments, that copper, most likely in the Cu(I) form, is transferred from Cu·DJ-1 to SOD1 and, through a SOD1 activity assay, that the transfer takes place toward the correct active SOD1 copper binding site, but we did not pursue a quantitative analysis of the transfer mechanism.

Specifically, we show that copper migrates from the Cys-106 copper binding site of DJ-1 to SOD1; accordingly, mutation of Cys-53 to alanine does not inhibit copper transfer to SOD1. We may therefore conclude from the absence of a functional effect that the Cu(I) binding site located between the two Cys-53 residues in the DJ-1 dimer may be related to a function different from the one described here (22, 32). We did not proceed further in the investigation of the specific function supported by this Cu(I) binding site, although it may be the one described by Bjorkblom *et al.* (22) (*i.e.* a direct metal sequestration to protect the system from metal-induced toxicity).

All of the described peculiar features of metal binding site 1 qualify DJ-1 as a metallochaperone, able to efficiently transfer copper to SOD1. Although DJ-1 is able to bind Cu(II) under oxidizing conditions, resulting in a green solution stable for at least 1 day at 4 °C, we showed, through x-ray crystallography, that it can also bind Cu(I). Moreover, DJ-1 seems to have the ability to favor copper reduction (x-ray absorption edge spectroscopy and x-ray data) so as to optimize copper transfer and avoid dangerous Cu(II) ions in solution. In fact, copper transporters bind almost invariably Cu(I) (46). The role of the network of residues surrounding Cys-106 seems to be fine tuning and defining the redox potential of Cys-106, which acts as a switch of the protein antioxidative defense mechanism also through the coupled activity with SOD1 (22).

The preferred route for SOD1 copper loading and activation is most likely through the copper chaperone for SOD1 (CCS) (47), whose mechanism of copper insertion and SOD1 activation has been elucidated (48–50). Initially, CCS was believed to represent the sole means to activate SOD1 *in vivo*, but later a CCS-independent pathway was postulated when it was shown that both CCS null *Drosophila* and mice models partially retained SOD1 activity (51, 52). Furthermore, the CCS gene is not present in all eukaryotes, whereas SOD1 is (53). It has also been suggested that the existence of a dual mechanisms for SOD1 activation may lie in its dual role of oxidative stress regulator and cell signaling factor. DJ-1 seems to act in the same pathways as SOD1, compensating and supporting both SOD1 roles. We may suggest that although DJ-1 is an atypical peroxiredoxin-like peroxidase, as also previously reported (42), under critical conditions, it can act also as a copper chaperone for SOD1 through a backup, CCS-independent pathway.

According to our results, the Cu·DJ-1 form is still able to retain its peroxiredoxin-like activity, allowing the protein to preserve at least a residual SOD1 activity under extreme conditions, such as hypoxia, when the CCS-dependent pathway is not working (54). The ability of DJ-1 to act in the CCS-independent activation pathway of SOD1 is still based on the presence of Cys-106, which is critical for both its peroxiredoxin-like activity and its copper chaperone function as well as for all of the functions ascribed so far to DJ-1 (5).

The recent report that DJ-1 binds metals such as copper and mercury (22), and in particular the specific binding at the dimer interface involving Cys-53 (site 2) (32), points to the potential role of DJ-1 in protecting the cell against metal-induced cytotoxicity. Although we identified site 2 as an actual Cu(I) binding site, we suggest that copper binding site 1, involving Cys-106, is the key site that allows the transfer of the metal to SOD1 under critical conditions. The latter function ascribed to the Cys-106 copper binding site could coexist with the function already suggested for the Cys-53 metal binding site (22, 32).

Through pull-down assays, Yamashita *et al.* (15) have already suggested the existence of a direct interaction between DJ-1 and SOD1. They showed the formation of complexes of mutant SOD1 and DJ-1 in mice primary motor neuron cultures. Moreover, the overexpression of exogenous DJ-1 in neuronal cells, stably expressing SOD1 mutants, showed increased cell viability and reduced cell toxicity due to reduced oxidative stress levels. A possible explanation of these results may be the ability of Cu·DJ-1 to rescue SOD1 activity in a critical situation, such as the one represented by SOD1 mutations, which may impair normal SOD1 activation through CCS.

As already reported, CCS-independent and CCS-dependent SOD1 activation pathways seem to use the same source of copper, such as glutathione complexes, and the only difference between the two mechanisms should lie at the level of disulfide bond oxidation, which seems to be fundamental for metal transfer and SOD1 activation through the CCS-dependent pathway. The awareness of a potential role for DJ-1 in the CCS-independent SOD1 activation pathway is only the first step in the investigation of a mechanism whose details are still unknown. The SOD1/DJ-1 interaction mechanism as well as the disulfide bond formation involved in the process needs to be further investigated to elucidate the entire SOD1 backup activation process.

REFERENCES

- Zhang, L., Shimoji, M., Thomas, B., Moore, D. J., Yu, S. W., Marupudi, N. I., Torp, R., Torgner, I. A., Ottersen, O. P., Dawson, T. M., and Dawson, V. L. (2005) Mitochondrial localization of the Parkinson's disease related protein DJ-1: implications for pathogenesis. *Hum. Mol. Genet.* **14**, 2063–2073
- Bonifati, V., Rizzu, P., van Baren, M. J., Schaap, O., Breedveld, G. J., Krieger, E., Dekker, M. C., Squitieri, F., Ibanez, P., Joosse, M., van Dongen, J. W., Vanacore, N., van Swieten, J. C., Brice, A., Meco, G., van Duijn, C. M., Oostra, B. A., and Heutink, P. (2003) Mutations in the DJ-1 gene associated with autosomal recessive early-onset parkinsonism. *Science* **299**, 256–259
- Waragai, M., Wei, J., Fujita, M., Nakai, M., Ho, G. J., Masliah, E., Akatsu, H., Yamada, T., and Hashimoto, M. (2006) Increased level of DJ-1 in the cerebrospinal fluids of sporadic Parkinson's disease. *Biochem. Biophys. Res. Commun.* **345**, 967–972

DJ-1 Is a Copper Chaperone Acting on SOD1 Activation

- Wilson, M. A., Collins, J. L., Hod, Y., Ringe, D., and Petsko, G. A. (2003) The 1.1-Å resolution crystal structure of DJ-1, the protein mutated in autosomal recessive early onset Parkinson's disease. *Proc. Natl. Acad. Sci. U.S.A.* **100**, 9256–9261
- Cookson, M. R. (2010) DJ-1, PINK1, and their effects on mitochondrial pathways. *Mov. Disord.* **25**, S44–S48
- Kahle, P. J., Waak, J., and Gasser, T. (2009) DJ-1 and prevention of oxidative stress in Parkinson's disease and other age-related disorders. *Free Radic. Biol. Med.* **47**, 1354–1361
- Canet-Avilés, R. M., Wilson, M. A., Miller, D. W., Ahmad, R., McLendon, C., Bandyopadhyay, S., Baptista, M. J., Ringe, D., Petsko, G. A., and Cookson, M. R. (2004) The Parkinson's disease protein DJ-1 is neuroprotective due to cysteine-sulfinic acid-driven mitochondrial localization. *Proc. Natl. Acad. Sci. U.S.A.* **101**, 9103–9108
- Kim, R. H., Smith, P. D., Aleyasin, H., Hayley, S., Mount, M. P., Pownall, S., Wakeham, A., You-Ten, A. J., Kalia, S. K., Horne, P., Westaway, D., Lozano, A. M., Anisman, H., Park, D. S., and Mak, T. W. (2005) Hypersensitivity of DJ-1-deficient mice to 1-methyl-4-phenyl-1,2,3,6-tetrahydropyridine (MPTP) and oxidative stress. *Proc. Natl. Acad. Sci. U.S.A.* **102**, 5215–5220
- Olzmann, J. A., Brown, K., Wilkinson, K. D., Rees, H. D., Huai, Q., Ke, H., Levey, A. I., Li, L., and Chin, L. S. (2004) Familial Parkinson's disease-associated L166P mutation disrupts DJ-1 protein folding and function. *J. Biol. Chem.* **279**, 8506–8515
- Kinumi, T., Kimata, J., Taira, T., Ariga, H., and Niki, E. (2004) Cysteine-106 of DJ-1 is the most sensitive cysteine residue to hydrogen peroxide-mediated oxidation *in vivo* in human umbilical vein endothelial cells. *Biochem. Biophys. Res. Commun.* **317**, 722–728
- Witt, A. C., Lakshminarasimhan, M., Remington, B. C., Hasim, S., Pozharzki, E., and Wilson, M. A. (2008) Cysteine pK_a depression by a protonated glutamic acid in human DJ-1. *Biochemistry* **47**, 7430–7440
- Giroto, S., Sturlese, M., Bellanda, M., Tessari, I., Cappellini, R., Bisaglia, M., Bubacco, L., and Mammi, S. (2012) Dopamine-derived quinones affect the structure of the redox sensor DJ-1 through modifications at Cys-106 and Cys-53. *J. Biol. Chem.* **287**, 18738–18749
- Bandyopadhyay, R., Kingsbury, A. E., Cookson, M. R., Reid, A. R., Evans, I. M., Hope, A. D., Pittman, A. M., Lashley, T., Canet-Avilés, R., Miller, D. W., McLendon, C., Strand, C., Leonard, A. J., Abou-Sleiman, P. M., Healy, D. G., Ariga, H., Wood, N. W., de Silva, R., Revesz, T., Hardy, J. A., and Lees, A. J. (2004) The expression of DJ-1 (PARK7) in normal human CNS and idiopathic Parkinson's disease. *Brain* **127**, 420–430
- Lev, N., Ickowicz, D., Barhum, Y., Melamed, E., and Offen, D. (2009) DJ-1 changes in G93A-SOD1 transgenic mice: implications for oxidative stress in ALS. *J. Mol. Neurosci.* **38**, 94–102
- Yamashita, S., Mori, A., Kimura, E., Mita, S., Maeda, Y., Hirano, T., and Uchino, M. (2010) DJ-1 forms complexes with mutant SOD1 and ameliorates its toxicity. *J. Neurochem.* **113**, 860–870
- Valentine, J. S., Doucette, P. A., and Zittin Potter, S. (2005) Copper-zinc superoxide dismutase and amyotrophic lateral sclerosis. *Annu. Rev. Biochem.* **74**, 563–593
- Noor, R., Mittal, S., and Iqbal, J. (2002) Superoxide dismutase: applications and relevance to human diseases. *Med. Sci. Monit.* **8**, RA210–RA215
- Bosco, D. A., Morfini, G., Karabacak, N. M., Song, Y., Gros-Louis, F., Pasinelli, P., Goolsby, H., Fontaine, B. A., Lemay, N., McKenna-Yasek, D., Frasch, M. P., Agar, J. N., Julien, J. P., Brady, S. T., and Brown, R. H., Jr. (2010) Wild-type and mutant SOD1 share an aberrant conformation and a common pathogenic pathway in ALS. *Nat. Neurosci.* **13**, 1396–1403
- Potter, S. Z., Zhu, H., Shaw, B. F., Rodriguez, J. A., Doucette, P. A., Sohn, S. H., Durazo, A., Faull, K. F., Gralla, E. B., Nersissian, A. M., and Valentine, J. S. (2007) Binding of a single zinc ion to one subunit of copper-zinc superoxide dismutase apoprotein substantially influences the structure and stability of the entire homodimeric protein. *J. Am. Chem. Soc.* **129**, 4575–4583
- Wang, Z., Liu, J., Chen, S., Wang, Y., Cao, L., Zhang, Y., Kang, W., Li, H., Gui, Y., Chen, S., and Ding, J. (2011) DJ-1 modulates the expression of Cu/Zn-superoxide dismutase-1 through the Erk1/2-Elk1 pathway in neuroprotection. *Ann. Neurol.* **70**, 591–599
- Xu, X. M., Lin, H., Maple, J., Björkblom, B., Alves, G., Larsen, J. P., and Møller, S. G. (2010) The *Arabidopsis* DJ-1a protein confers stress protection through cytosolic SOD activation. *J. Cell Sci.* **123**, 1644–1651
- Björkblom, B., Adilbayeva, A., Maple-Grødem, J., Piston, D., Ökvist, M., Xu, X. M., Brede, C., Larsen, J. P., and Møller, S. G. (2013) Parkinson disease protein DJ-1 binds metals and protects against metal-induced cytotoxicity. *J. Biol. Chem.* **288**, 22809–22820
- Carlioz, A., and Touati, D. (1986) Isolation of superoxide dismutase mutants in *Escherichia coli*: is superoxide dismutase necessary for aerobic life? *EMBO J.* **5**, 623–630
- Banci, L., Bertini, I., Durazo, A., Giroto, S., Gralla, E. B., Martinelli, M., Valentine, J. S., Vieru, M., and Whitelegge, J. P. (2007) Metal-free superoxide dismutase forms soluble oligomers under physiological conditions: a possible general mechanism for familial ALS. *Proc. Natl. Acad. Sci. U.S.A.* **104**, 11263–11267
- Banci, L., Benedetto, M., Bertini, I., Del Conte, R., Piccioli, M., and Viezzoli, M. S. (1998) Solution structure of reduced monomeric Q133M2 copper, zinc superoxide dismutase (SOD). Why is SOD a dimeric enzyme? *Biochemistry* **37**, 11780–11791
- McCord, J. M., and Fridovich, I. (1969) Superoxide dismutase. An enzymic function for erythrocyte hemocuprein. *J. Biol. Chem.* **244**, 6049–6055
- Forman, H. J., and Fridovich, I. (1973) On the stability of bovine superoxide dismutase. The effects of metals. *J. Biol. Chem.* **248**, 2645–2649
- Collaborative Computational Project, Number 4 (1994) The CCP4 suite: programs for protein crystallography. *Acta Crystallogr. D Biol. Crystallogr.* **50**, 760–763
- Adams, P. D., Afonine, P. V., Bunkóczi, G., Chen, V. B., Davis, I. W., Echols, N., Headd, J. J., Hung, L. W., Kapral, G. J., Grosse-Kunstleve, R. W., McCoy, A. J., Moriarty, N. W., Oeffner, R., Read, R. J., Richardson, D. C., Richardson, J. S., Terwilliger, T. C., and Zwart, P. H. (2010) PHENIX: a comprehensive Python-based system for macromolecular structure solution. *Acta Crystallogr. D Biol. Crystallogr.* **66**, 213–221
- Murshudov, G. N., Skubák, P., Lebedev, A. A., Pannu, N. S., Steiner, R. A., Nicholls, R. A., Winn, M. D., Long, F., and Vagin, A. A. (2011) REFMAC5 for the refinement of macromolecular crystal structures. *Acta Crystallogr. D Biol. Crystallogr.* **67**, 355–367
- Emsley, P., and Cowtan, K. (2004) Coot: model-building tools for molecular graphics. *Acta Crystallogr. D Biol. Crystallogr.* **60**, 2126–2132
- Puno, M. R., Patel, N. A., Møller, S. G., Robinson, C. V., Moody, P. C., and Odell, M. (2013) Structure of Cu(I)-bound DJ-1 reveals a biscysteinate metal binding site at the homodimer interface: insights into mutational inactivation of DJ-1 in parkinsonism. *J. Am. Chem. Soc.* **135**, 15974–15977
- Corbett, M. C., Latimer, M. J., Poulos, T. L., Sevrioukova, I. F., Hodgson, K. O., and Hedman, B. (2007) Photoreduction of the active site of the metalloprotein putidaredoxin by synchrotron radiation. *Acta Crystallogr. D Biol. Crystallogr.* **63**, 951–960
- Baker, E. N. (1988) Structure of azurin from *Alcaligenes denitrificans* refinement at 1.8 Å resolution and comparison of the two crystallographically independent molecules. *J. Mol. Biol.* **203**, 1071–1095
- Durley, R., Chen, L., Lim, L. W., Mathews, F. S., and Davidson, V. L. (1993) Crystal structure analysis of amicyanin and apoamicyanin from *Paracoccus denitrificans* at 2.0 Å and 1.8 Å resolution. *Protein Sci.* **2**, 739–752
- Lacroix, J. S., Ricchetti, A. P., Morel, D., Mossimann, B., Waerber, B., and Grouzmann, E. (1996) Intranasal administration of neuropeptide Y in man: systemic absorption and functional effects. *Br. J. Pharmacol.* **118**, 2079–2084
- Shepard, W. E., Kingston, R. L., Anderson, B. F., and Baker, E. N. (1993) Structure of apo-azurin from *Alcaligenes denitrificans* at 1.8 Å resolution. *Acta Crystallogr. D Biol. Crystallogr.* **49**, 331–343
- Banci, L., Bertini, I., Ciofi-Baffoni, S., Huffman, D. L., and O'Halloran, T. V. (2001) Solution structure of the yeast copper transporter domain Ccc2a in the apo and Cu(I)-loaded states. *J. Biol. Chem.* **276**, 8415–8426
- Banci, L., Bertini, I., Del Conte, R., D'Onofrio, M., and Rosato, A. (2004) Solution structure and backbone dynamics of the Cu(I) and apo forms of the second metal-binding domain of the Menkes protein ATP7A. *Biochemistry* **43**, 3396–3403
- DeSilva, T. M., Veglia, G., and Opella, S. J. (2005) Solution structures of the reduced and Cu(I) bound forms of the first metal binding sequence of

- ATP7A associated with Menkes disease. *Proteins* **61**, 1038–1049
41. Blackinton, J., Lakshminarasimhan, M., Thomas, K. J., Ahmad, R., Greggio, E., Raza, A. S., Cookson, M. R., and Wilson, M. A. (2009) Formation of a stabilized cysteine sulfinic acid is critical for the mitochondrial function of the parkinsonism protein DJ-1. *J. Biol. Chem.* **284**, 6476–6485
 42. Andres-Mateos, E., Perier, C., Zhang, L., Blanchard-Fillion, B., Greco, T. M., Thomas, B., Ko, H. S., Sasaki, M., Ischiropoulos, H., Przedborski, S., Dawson, T. M., and Dawson, V. L. (2007) DJ-1 gene deletion reveals that DJ-1 is an atypical peroxiredoxin-like peroxidase. *Proc. Natl. Acad. Sci. U.S.A.* **104**, 14807–14812
 43. Trempe, J. F., and Fon, E. A. (2013) Structure and function of Parkin, PINK1, and DJ-1, the three musketeers of neuroprotection. *Front. Neurol.* **4**, 38
 44. Rosato, N., Mei, G., Gratton, E., Bannister, J. V., Bannister, W. H., and Finazzi-Agrò, A. (1990) A time-resolved fluorescence study of human copper-zinc superoxide dismutase. *Biophys. Chem.* **36**, 41–46
 45. Szabo, A. G., Stepanik, T. M., Wayner, D. M., and Young, N. M. (1983) Conformational heterogeneity of the copper binding site in azurin. A time-resolved fluorescence study. *Biophys. J.* **41**, 233–244
 46. Banci, L., Bertini, I., and Ciofi-Baffoni, S. (2009) Copper trafficking in biology: an NMR approach. *HFSP J.* **3**, 165–175
 47. Culotta, V. C., Klomp, L. W., Strain, J., Casareno, R. L., Krems, B., and Gitlin, J. D. (1997) The copper chaperone for superoxide dismutase. *J. Biol. Chem.* **272**, 23469–23472
 48. Furukawa, Y., and O'Halloran, T. V. (2006) Posttranslational modifications in Cu,Zn-superoxide dismutase and mutations associated with amyotrophic lateral sclerosis. *Antioxid. Redox Signal.* **8**, 847–867
 49. Lamb, A. L., Torres, A. S., O'Halloran, T. V., and Rosenzweig, A. C. (2001) Heterodimeric structure of superoxide dismutase in complex with its metallochaperone. *Nat. Struct. Biol.* **8**, 751–755
 50. Schmidt, P. J., Rae, T. D., Pufahl, R. A., Hamma, T., Strain, J., O'Halloran, T. V., and Culotta, V. C. (1999) Multiple protein domains contribute to the action of the copper chaperone for superoxide dismutase. *J. Biol. Chem.* **274**, 23719–23725
 51. Wong, P. C., Waggoner, D., Subramaniam, J. R., Tessarollo, L., Bartnikas, T. B., Culotta, V. C., Price, D. L., Rothstein, J., and Gitlin, J. D. (2000) Copper chaperone for superoxide dismutase is essential to activate mammalian Cu/Zn superoxide dismutase. *Proc. Natl. Acad. Sci. U.S.A.* **97**, 2886–2891
 52. Kirby, K., Jensen, L. T., Binnington, J., Hilliker, A. J., Ulloa, J., Culotta, V. C., and Phillips, J. P. (2008) Instability of superoxide dismutase 1 of *Drosophila* in mutants deficient for its cognate copper chaperone. *J. Biol. Chem.* **283**, 35393–35401
 53. Jensen, L. T., and Culotta, V. C. (2005) Activation of CuZn superoxide dismutases from *Caenorhabditis elegans* does not require the copper chaperone CCS. *J. Biol. Chem.* **280**, 41373–41379
 54. Brown, N. M., Torres, A. S., Doan, P. E., and O'Halloran, T. V. (2004) Oxygen and the copper chaperone CCS regulate posttranslational activation of Cu,Zn superoxide dismutase. *Proc. Natl. Acad. Sci. U.S.A.* **101**, 5518–5523

DJ-1 Is a Copper Chaperone Acting on SOD1 Activation

Stefania Giroto, Laura Cendron, Marco Bisaglia, Isabella Tessari, Stefano Mammi,
Giuseppe Zanotti and Luigi Bubacco

J. Biol. Chem. 2014, 289:10887-10899.

doi: 10.1074/jbc.M113.535112 originally published online February 24, 2014

Access the most updated version of this article at doi: [10.1074/jbc.M113.535112](https://doi.org/10.1074/jbc.M113.535112)

Alerts:

- [When this article is cited](#)
- [When a correction for this article is posted](#)

[Click here](#) to choose from all of JBC's e-mail alerts

This article cites 54 references, 22 of which can be accessed free at
<http://www.jbc.org/content/289/15/10887.full.html#ref-list-1>